Turbulence in a wedge: The case of the mixing layer

Yves Pomeau and Martine Le Berre
Laboratoire d'Hydrodynamique, Ladhyx, CNRS UMR 7646, Ecole Polytechnique, 91128 Palaiseau, France

(Received 23 December 2020; accepted 9 June 2021; published 6 July 2021)

The ultimate goal of a sound theory of turbulence in fluids is to close in a rational way the Reynolds equations, namely, to express the tensor of turbulent stress as a function of the time average of the velocity field. Based on the idea that dissipation in fully developed turbulence is by singular events resulting from an evolution described by the Euler equations, it has been recently observed that the closure problem is strongly restricted, and that it implies that the turbulent stress is a nonlocal function in space of the average velocity field, a kind of extension of classical Boussinesq theory of turbulent viscosity. This leads to rather complex nonlinear integral equation(s) for the time-averaged velocity field. This one satisfies some symmetries of the Euler equations. Such symmetries were used by Prandtl and Landau to make various predictions about the shape of the turbulent domain in simple geometries. We explore specifically the case of the mixing layer for which the average velocity field only depends on the angle of the wedge behind the splitter plate. This solution yields a pressure difference between the two sides of the splitter which contributes to the lift felt by the plate. Moreover, because of the structure of the equations, one can satisfy the Cauchy-Schwarz inequalities for the turbulent stress, also called the realizability conditions. In the limit of small velocity differences between the two merging flows behind the splitter, we predict an angular spreading of the turbulent domain proportional to the square root of the velocity difference, in agreement with experiments.

DOI: 10.1103/PhysRevFluids.6.074603

I. INTRODUCTION

One fundamental result in fluid mechanics goes back to Newton's Principia and states that at large constant velocity (large Reynolds number in modern terms) the drag force on a blunt body is proportional to the product of the square of its velocity, the cross section, and the mass density of the fluid. This remarkable result is not trivial, because it is fully independent of the viscosity, that is *a priori* responsible for the dissipation in fluids. An explanation is that dissipation takes place in singular events [1] resulting from the evolution described by Euler inviscid equations. Although viscosity becomes relevant in the final stage of this evolution, the amount of energy dissipated there is independent of the viscosity, because it is the energy present both initially and in the final stage of the singular solution which is fully described by the energy-conserving Euler dynamics [2,3]. This explanation based on singular events is the one we adopt here following Ref. [4], where it was shown that this approach leads to an expression of the turbulent stress tensor formulated in terms of the time-averaged velocity field, which is nonlocal in space. The nonlocality follows from the constraint that all physical parameters depend on the average velocity field; i.e., they are not adjusted to experiments. This constraint is the key leading to our model for the Reynolds stress tensor (RST), defined by the correlation of the velocity fluctuations $\mathbf{U}'$ by the relation (neglecting the contribution of the viscous stress)

$$\sigma_{ij}^{\mathrm{Re}}(\mathbf{X}) = \rho\langle U_i'(\mathbf{X})U_j'(\mathbf{X})\rangle, \tag{1}$$

where $\langle\cdot\rangle$ means a *time average*. Defining $U(\mathbf{X})$ (without brackets in order to lighten the writing) as the time average of the velocity, our nonlocal model for the Reynolds stress belongs to the class of equations written as the sum of two contributions

$$\sigma_{ij}^{\mathrm{Re}}(\mathbf{X}) = \tilde{\sigma}_{ij}^{\mathrm{Re}}(\mathbf{X}) + \sigma_{ij}^{\mathrm{Re},p}(\mathbf{X}), \tag{2}$$

where the second term is the nondiagonal tensor

$$\tilde{\sigma}_{ij}^{\mathrm{Re}}(\mathbf{X}) = \tilde{\gamma}\rho|\nabla\times\mathbf{U}(\mathbf{X})|^{1-\alpha}\int d\mathbf{X}'|\nabla\times\mathbf{U}(\mathbf{X}')|^{\alpha}\left(\frac{1}{|\mathbf{X}-\mathbf{X}'|}-\frac{1}{|\mathbf{X}'|}\right)(U_{i,j}+U_{j,i})(\mathbf{X}') \tag{3}$$

and the second term on the right-hand side (rhs) of Eq. (2) is the diagonal tensor

$$\sigma_{ij}^{\mathrm{Re},p}(\mathbf{X}) = \delta_{ij}\gamma\rho|\nabla\times\mathbf{U}(\mathbf{X})|^{1-\alpha}\int d\mathbf{X}'|\nabla\times\mathbf{U}(\mathbf{X}')|^{\alpha+1}\left(\frac{1}{|\mathbf{X}-\mathbf{X}'|}-\frac{1}{|\mathbf{X}'|}\right). \tag{4}$$

In Eqs. (3) and (4) the exponent α is such that $0<\alpha<1$, and $\tilde{\gamma}$ and γ are dimensionless constants. Those three quantities have to be found either by analyzing experimental results and/or numerical simulations. In Eq. (2) the indices i and j are for the Cartesian coordinates, and δ_{ij} is the Kronecker symbol. They should not be confused with the two indices 1 and 2 attributed to the two sides of the mixing layer later in this paper. Above and elsewhere we use the notation with a comma in the subscript to denote derivation, so that $U_{i,j}$ is for $\frac{\partial U_i}{\partial X_j}$.

Our model is not derived from the full unclosed rate equation for the Reynolds stress tensor because this would require to know how singular events appear in incompressible Newtonian flows, an open question to date. Let us explain the way the Reynolds stress $\sigma_{ij}^{\mathrm{Re}}$ is built. As one can check it has the same scaling properties as the turbulent stress imagined long ago by Boussinesq; namely, it scales like velocity square times ρ. However, it has some features requiring to be explained. The first obvious feature of this equation is that it is obviously not invariant under spatial translation, because the counter term $\frac{1}{|\mathbf{X}'|}$ in the integral kernel introduces an (unspecified) origin of coordinates from which the vector $\mathbf{X}'$ is measured. This breaking of the translational invariance is not surprising by itself, because the turbulent Reynolds stress depends on the average properties of the turbulent fluctuations (see below), which depend on the geometry of the walls limiting the fluid. In the case of a fluid bounded by walls, an extended version of the integral kernel is to take the Green's function of the Laplace operator with Dirichlet boundary conditions. This would amount to replace in Eqs. (3) and (4) the integral kernel $(\frac{1}{|\mathbf{X}-\mathbf{X}'|}-\frac{1}{|\mathbf{X}'|})$ by $K(\mathbf{X},\mathbf{X}')$, where K is the solution of Laplace's equation with respect to the variable X:

$$\nabla^2 K(\mathbf{X},\mathbf{X}') = \delta_{\mathrm{D}}(\mathbf{X}-\mathbf{X}'), \tag{5}$$

where δ_{D} is Dirac's delta function. The solution of Eq. (5) must satisfy the boundary condition that the turbulent stress vanishes on the solid surfaces limiting the fluid. Generally speaking, one of the many questions raised by turbulence modeling is precisely the way boundary conditions for the stress are imposed. In the present theory this is done thanks to the (nontrivial) choice of the kernel $K(X,X')$, which depends on the geometry of the turbulent flow.

Here we deal with the mixing layer setup where a half-infinite splitting plate ends up on the line defined by the Cartesian equation $x=y=0$ (see Fig. 1). Because this mixing layer has a simple geometry it is natural to take as the origin of the coordinates a point on the edge of the splitter, as we do. This is justified by the fact that, without this counter term in the integral equation, the integral (over the variable z, along the edge of the splitter) diverges logarithmically. Subtracting this counter term one finds a converging result because the divergence of the two terms cancels each other. Moreover, including this counter term, the turbulent stress scales like the product of ρ by the square of a velocity square. More complex physical situations, like the one of a turbulent flow around an obstacle like a sphere or a turbulent Poiseuille pipe flow, require to introduce the more complex integral kernel $K(\mathbf{X},\mathbf{X}')$ defined by Eq. (5), because a significant question is the convergence of the integral in Eq. (3). Given that the integrand of Eq. (3) is proportional to the

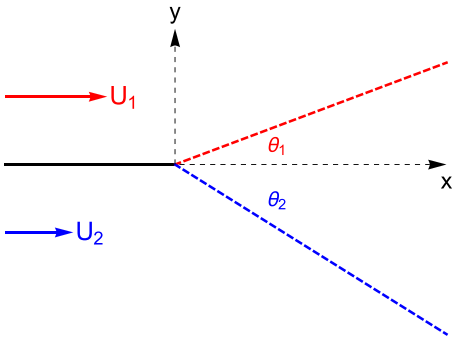

FIG. 1. Cross section of a mixing layer in the plane (x, y). The obstacle is a semi-infinite plane, located in the domain $(x < 0, -\infty < z < \infty)$; the incident flow has different velocities U_1 and U_2 above and below the obstacle. Behind the obstacle, a turbulent wedge is formed, materialized by the two rays making angles θ_1 and θ_2 with the x axis (in Landau's description the flow is nonpotential inside this wedge).

fraction $1/|\mathbf{X} - \mathbf{X}'|$, this integral may be diverging at large values of $|\mathbf{X}'|$ depending on how the rest of the integrand behaves in this limit. For instance, if this integrand depends on a single Cartesian coordinate of $\mathbf{X}'$, the integral diverges logarithmically, a divergence that is canceled by subtracting $1/|\mathbf{X}'|$ from $1/|\mathbf{X} - \mathbf{X}'|$ as done here. However, this implies a choice of origin of coordinates that is not always possible in other geometries. For a Poiseuille flow in a circular pipe or between two parallel plates, any choice of the origin of coordinates along the pipe will break the translational symmetry in the direction of the flow. Therefore, one has to replace in those cases $1/|\mathbf{X} - \mathbf{X}'|$ by the Green's function $K(\mathbf{X}, \mathbf{X}')$ solution of Eq. (5) [5].

Another property of expressions (3) and (4) for the turbulent stress is the explicit occurrence of the vorticity. Vorticity is known to play a central role in nonhomogeneous and nonisotropic turbulence, because once vorticity is present, it is amplified by vortex stretching. Moreover, our model agrees with Landau's description of wakes (Sec. 35 in Ref. [6]), made up of two domains, one potential and the other rotational. In the rotational (nonpotential) domain there is a kind of equilibrium on average between the growth of vorticity, by vortex stretching and by injection from the boundaries, and its damping in singular events. About the potential domain, Landau states that "outside the region of rotational flow, the turbulent eddies must be damped and must be so more rapidly for small eddies which do not penetrate far away in the potential domain (Sec. 36, p. 146, 2nd ed.)."

Expression (3) agrees with the basic constraints derived from the structure of Euler fluid equations, except for the one of reversibility (which constrains smooth solutions but not singular ones). We emphasize that a strong point of our paper is to introduce irreversibility in the Reynolds stress tensor associated to Euler equations, because our starting point is that dissipation occurs at singular events. This approach differs from standard Reynolds-averaged Navier-Stokes (RANS) models where irreversibility is introduced via the dynamics of a dissipation field, which is questionable for Euler equations. Indeed, as is well known, this dissipation field yields a nonsmooth velocity field of Holder exponent $1/3$ which excludes the writing of differential equation for its dynamics, particularly because the $(\boldsymbol{u} \cdot \mathrm{grad}\, \boldsymbol{u})$ term becomes very singular at short distance if this scaling is correct (something we do not believe; see our study based on Modane's data in Ref. [2]).

Irreversibility is attached to expression (14) of the full stress tensor, where the first term of the RST is the product of absolute value of the vorticity by the strain tensor components, which makes the turbulent stress $\tilde{\sigma}_{ij}^{\mathrm{Re}}$ change sign when changing the sign of U, whereas the inertia stress $\rho U_i U_j$ and $\sigma_{ij}^{\mathrm{Re},p}$ do not change sign. In our picture of turbulence the irreversibility is due to the evolution toward finite time singularities of the Leray type [1], the solution disappearing close to the collapse time due to molecular dissipation at small scales, so that dissipation will ultimately yield the friction

of Newton's drag law. This picture of dissipation at collapse time is analogous to Maxwell's theory of the molecular viscosity of gases [7], where the velocity difference between two colliding particles induced by a macroscopic shear flow reduces to zero when the particles collide, transforming the energy of this velocity difference into heat. As just written, $\sigma_{ij}^{\mathrm{Re},p}$ does not change sign as $\mathbf{U}$ changes sign. Therefore, the addition of $\sigma^{\mathrm{Re},p}$ to turbulent stress will represent a contribution to this stress that does not participate in friction, that is possible *a priori*. In particular in the geometry of the mixing layer, the $\sigma_{zz}^{\mathrm{Re}}$ component of the stress cannot enter into the friction which, by symmetry, is a force directed along the x axis. Therefore, dissipation must depend only on the $\sigma_{ij}^{\mathrm{Re}}$ components with at least one index i or j equal to x, that excludes $\sigma_{zz}^{\mathrm{Re}}$.

Let us return to the nonlocal property of our model. The nonlocality has a double origin: one is the time-averaging process that defines the RST components $\langle U_i'(\mathbf{X})U_j'(\mathbf{X})\rangle$ and the velocity $\mathbf{U}$; the other is related to the nonlocal equation for the pressure. However, the latter point (pressure) is not essential in our model (see below), although it is so in the strategy for closure in RANS models. Our interpretation is rather than nonlocality is due to the time-averaging process which amounts to considering that the velocity fluctuations U_j' propagate information from one point to others, which give expressions of the RST components depending on the mean velocity $\mathbf{U}$ (time average) at spatial points different from those where the RST is calculated.

Let us now explain why we add the diagonal tensor $\sigma_{ij}^{\mathrm{Re},p}$ to the tensor $\tilde{\sigma}_{ij}^{\mathrm{Re}}$ ($\sigma_{ij}^{\mathrm{Re},p}$ was not added in our previous paper [4]). This is done because the trace of $\tilde{\sigma}_{ij}^{\mathrm{Re}}$ is proportional to the divergence of the velocity field, $\nabla\cdot\mathbf{U} = U_{i,i}$ (with summation on repeated indices), which is zero for incompressible fluids. The null trace of the tensor $\tilde{\sigma}_{ij}^{\mathrm{Re}}$ is not compatible with the definition of the Reynolds stress tensor in Eq. (1) which implies that all diagonal elements must be positive, and must be related to the off-diagonal elements by the Schwarz inequality [see Eq. (F7) in Appendix F, these two conditions being named realizability condition [8]).

In our model the diagonal tensor $\sigma_{ij}^{\mathrm{Re},p}$ plays the role of a time-averaged pressure, called *turbulent pressure* below. Let us notice that the trace of the diagonal tensor $\sigma_{ij}^{\mathrm{Re},p}$, which is twice the turbulent kinetic energy, is caused by the vorticity and depends on the spatial coordinates, although it is assumed to be constant, equal to the dissipation rate ϵ, in the case of homogeneous and isotropic turbulence, giving rise, for instance, to the eddy-viscosity-based models like the k-ϵ and the k-ω models. This tensor $\sigma_{ij}^{\mathrm{Re},p}$ has to be added to the usual time-averaged pressure (also spatially dependent) which exists without vorticity. Recall that in dynamical equations for incompressible inviscid flows the pair $(\mathbf{U}, p)$ is not unique, because p is a scalar gauge field defined up to an additive constant. In other words the pressure is not an independent variable, but a Lagrangian multiplier necessary to ensure the compressibility, since it fulfills the relation $\nabla p = \mathbf{U}_{i,j}\mathbf{U}_{j,i}$. In the mixing layer case with quasiequal incoming velocities the conditions are fulfilled by taking equal coefficients $\tilde{\gamma} = \gamma$ in Eqs. (3) and (4). In other cases we expect that the factor γ in turbulent pressure can be adjusted to satisfy the constraints of the realizability. Actually the turbulent pressure is not used below for the calculation of the components U_i; it is just introduced to ensure that the realizability conditions are fulfilled (see Sec. III B 2).

In summary, our model of the Reynolds stress contains a part which is linear with respect to the strain tensor τ_{ij} plus the turbulent pressure,

$$p^{\mathrm{turb}} = \sigma_{ii}^{\mathrm{Re},p}, \tag{6}$$

whose source is the vorticity [see Eq. (4)]. The link between the pressure and the vorticity is also in agreement with the fact that turbulence is characterized by vorticity in real turbulent flows. Note that it is well known that vorticity is a source of low pressure in incompressible fluids, irrespective of the sign of the vorticity, which makes the turbulent wake domain suck part of the flow of the potential domain, leading for example to the Coanda effect [9]. The interest of introducing this turbulent pressure will hopefully be more obvious in the case of the turbulent mixing layer studied below. First we solve the equation for the balance of momentum by eliminating the scalar pressure,

which allows to obtain an analytical expression for the average velocity field. In a second step we set an expression for the total scalar pressure,

$$p_t = p^{\text{turb}} + p, \tag{7}$$

including the average of the standard thermodynamical pressure p (associated to the so-called RANS equation) and the turbulent pressure. The latter is computed by using Eq. (4), and the standard pressure is the difference between the total pressure and the turbulent pressure.

The present work is mainly devoted to the application of the model of turbulence, Eqs. (3) and (4), to a given situation, and so we leave aside a discussion about their validity as compared to existing models of turbulence [10] developed after the seminal paper of Launder *et al.* [11]. We emphasize that conventional Reynolds-averaged Navier-Stokes modeling for the Reynolds stress is mostly designed for numerical applications although we present here analytical results for the mixing layer (with two incident velocities along the plate) where turbulence is localized in a thin wedge behind a semi-infinite plate. As written above, the lack of knowledge of singular solutions for Euler equations, which are (in our opinion) responsible for the dissipation in the limit of large Reynolds number, impedes to derive a Reynolds stress model directly from Navier-Stokes or Euler equations. One can hope that one day the understanding of singular events will be good enough to derive a model from the Reynolds stress tensor full equation, but one has to be patient since it took about 300 years to progress from Newton' s viscosity idea, to Stokes and Navier's formatting and finally complete justification by Enskog (for gas) and by Green-Kubo for dense fluids.

Let us notice that a first difficulty met when trying to compare the present model with other models of turbulence with transport equations for averaged quantities is that those models give access in principle to time-dependent fluctuations. As our model is essentially a model for time-averaged quantities, a comparison would imply to choose to compare with the time average of the transported quantities or their instantaneous value. Another difficulty is that we aim at modeling the infinite Reynolds number limit whereas the Reynolds number of the time-dependent simulations is finite, usually in the range of a few hundreds, arguably quite different from the infinite Reynolds limit. Lastly many different models of turbulence exist with fairly different equations, showing perhaps that the last word has not been said in this field. In this respect a comparison of our results for the mixing layer with experiments and/or direct numerical simulations without modeling would be significant. Note in particular our clear prediction for the dependence of the spreading angle with respect to small velocity differences.

Below we consider the case of the mixing layer where the equations written in polar coordinates depend on one variable only, the angle. Section II is devoted to the relatively nontrivial task of writing Eq. (3) fully explicitly and to derive the equation for the balance of the total stress Σ_{ij} resulting from it, this tensor being the sum of the turbulent stress, the pressure, and the inertia stress [see Eq. (14)]. In Sec. III we solve this problem for a small velocity difference of the two merging flows. The details of the calculations are postponed to the Appendixes in order to lighten the main part of the paper.

II. FORMULAS IN POLAR COORDINATES

In this section we derive in polar coordinates the explicit equation for the balance of stress. The whole calculation is fairly complex and is done by using mixed coordinates, polar coordinates for the argument of the functions, and Cartesian coordinates for the velocity field and the stress tensor.

A. Stress balance in polar coordinates

We consider the turbulent wake behind a semi-infinite plane board (the splitter) supposed to be horizontal in the plane (x, z), limited to the domain $x < 0$, and submitted to two inviscid parallel flows with different velocities in the x direction, the upper one with velocity $\mathbf{U}_1$ and the

lower one with velocity $\mathbf{U}_2$, schematized in Fig. 1. No fluid parameter depends on the coordinate z perpendicular to the plane (x, y).

Because of symmetries of the equations and of the geometry, the time average of the velocity depends on the angle only, which leads us to use cylindrical coordinates (r, θ, z). The present derivation can be extended to other flow geometries where the velocity field depends on an angle only, like, for instance, a uniform parallel flow impinging an inclined plate at high Reynolds number. This assumption of a large Reynolds number implies that we consider what happens at distances from the splitter large enough to make the corresponding Reynolds number large. In this limit viscous effects as negligible so that, as had been shown by Prandtl, the average velocity in this plane depends on the polar angle θ only, with θ increasing from $\theta = 0$ on the x axis, to $\pi/2$ on the vertical axis y, to π on the upper part of the plate and symmetrically to $-\pi$ on the lower part. Setting $\theta = 0$ on the x axis, the coordinates x and y are related to the angle θ and the radius r by

$$x = r\cos\theta, \tag{8}$$

$$y = r\sin\theta. \tag{9}$$

The incompressible time-averaged velocity field $\mathbf{U}$ is in the plane (x, y) and is given by the stream function $\Psi = rg(\theta)$, where the function $g(\theta)$ is to be found. Let the Cartesian components of the velocity $\mathbf{U}$ be $U_x = u$ and $U_y = v$ in the directions x and y, respectively. From $u = -\Psi_{,y}$ and $v = \Psi_{,x}$ where the comma denotes partial derivatives, one has

$$u = -(g\sin\theta + g'\cos\theta), \tag{10}$$

$$v = g\cos\theta - g'\sin\theta, \tag{11}$$

where $g' = \frac{dg}{d\theta}$. Hopefully, no confusion will arise between this symbol of derivation and the primed notation X' for coordinates in Eqs. (3) and (4) and below in Eq. (13). The z component of the curl of the velocity field is the only nonvanishing component of the vorticity given by

$$\nabla \times \mathbf{U}(\mathbf{X}) = \frac{1}{r}(g + g'')\mathbf{e}_z, \tag{12}$$

where $g'' = \frac{d^2g}{d\theta^2}$ and $\mathbf{e}_z$ is the unit vector along z.

The integration over the coordinate z' in Eqs. (3) and (4) can be performed because the variable z' occurs only in the denominators in $\frac{1}{|\mathbf{X}-\mathbf{X}'|} - \frac{1}{|\mathbf{X}'|}$. The result is

$$\int dz' \left(\frac{1}{|\mathbf{X} - \mathbf{X}'|} - \frac{1}{|\mathbf{X}'|} \right) = \ln \left[\frac{a(r, r', \theta - \theta')}{a(0, r', \theta - \theta')} \right]^2, \tag{13}$$

where

$$a^2(r, r', \theta - \theta') = r^2 + r'^2 - 2rr'\cos(\theta - \theta').$$

The next step in this calculation is to write explicitly the condition of balance of momentum. Let us define the full stress tensor Σ_{ij}, which is the sum of three terms involving the contribution of inertia, Reynolds stress, and pressure $p\delta_{ij}$:

$$\Sigma_{ij} = \rho\, U_i U_j + \sigma_{ij}^{\mathrm{Re}} + p\delta_{ij}. \tag{14}$$

Within our model (2) it can also be written in the form

$$\Sigma_{ij} = \rho\, U_i U_j + \tilde{\sigma}_{ij}^{\mathrm{Re}} + (p + p^{\mathrm{turb}})\delta_{ij}, \tag{15}$$

which is the one used below in order to get the expression of the average velocity as a function of θ. In Cartesian coordinates the balance of momentum, which does not depend on z, is given by the

two conditions

$$\Sigma_{xx,x} + \Sigma_{xy,y} = 0 \tag{16}$$

and

$$\Sigma_{yy,y} + \Sigma_{xy,x} = 0. \tag{17}$$

In polar coordinates Eqs. (16) and (17) become the two following ordinary differential equations (ODEs) with respect to the variable θ:

$$-(\sin\theta)\Sigma_{xx,\theta} + (\cos\theta)\Sigma_{xy,\theta} = 0, \tag{18}$$

$$(\cos\theta)\Sigma_{yy,\theta} - (\sin\theta)\Sigma_{xy,\theta} = 0. \tag{19}$$

Let us consider the contributions of the first two terms in Eq. (15) up to a global multiplication by the mass density ρ that will not be written explicitly. The contribution of U_iU_j is expressed simply in terms of the stream function as

$$U_x^2 = u^2 = (g\sin\theta + g'\cos\theta)^2, \tag{20}$$

$$U_y^2 = v^2 = (g\cos\theta - g'\sin\theta)^2, \tag{21}$$

$$U_xU_y = uv = \sin\theta\cos\theta(g'^2 - g^2) + gg'(\sin^2\theta - \cos^2\theta). \tag{22}$$

At this step the unknown functions are $g(\cdot)$ and the pressure p, depending both on θ only. It is possible to eliminate the pressure by taking the curl of the two ODEs for the stress tensor, as usually done in this kind of problem. However, in the present case one more step can be made because the tensor Σ_{ij} and the pressure p depend on θ only. It follows that the pressure appears by its derivative with respect to θ only, in Eqs. (18) and (19). Therefore, one can eliminate the pressure from those equations by algebraic handling, without increasing the order of derivation in the final equation. Let us define $\tilde{\Sigma}_{ij}$ as Σ_{ij} without the total pressure term defined in Eq. (7):

$$\Sigma_{ij} = \tilde{\Sigma}_{ij} + p_t\delta_{ij}. \tag{23}$$

After straightforward algebra the components of $\tilde{\Sigma}_{ij}$ satisfy the following single equation without the pressure, and with $g(\theta)$ as the single unknown function:

$$\sin\theta\cos\theta(\tilde{\Sigma}_{yy,\theta} - \tilde{\Sigma}_{xx,\theta}) + (\cos^2\theta - \sin^2\theta)\tilde{\Sigma}_{xy,\theta} = 0, \tag{24}$$

which is the basic equation to be solved. Recall that the stress $\tilde{\Sigma}_{ij}$ is the sum of the inertia term U_iU_j plus the stress tensor $\tilde{\sigma}_{ij}^{\mathrm{Re}}$ given in Eq. (3), both being a function of the time-averaged velocity field and ultimately of the stream function of the same averaged velocity $\Psi = rg(\theta)$, $g(\cdot)$ being the unknown function to be found by solving Eq. (24). From the computational point of view, Eq. (24) is formally independent of the isotropic part of the stress, coming from the pressure. Either Eq. (18) or Eq. (19) can be used to find the total pressure, both equations being compatible because of the way Eq. (24) is derived. Using polar coordinates, Eqs. (18) and (19) lead to the relation

$$\frac{1}{\rho}(p_t)_{,\theta} = -\sin^2\theta\ \tilde{\Sigma}_{xx,\theta} - \cos^2\theta\ \tilde{\Sigma}_{yy,\theta} + 2\sin\theta\cos\theta\ \tilde{\Sigma}_{xy,\theta}. \tag{25}$$

Looking at the literature on the theory of the mixing layer one finds often a somewhat expeditious treatment of the pressure gradient which is set rather arbitrarily to zero. This seems not justified at least for a number of reasons. First, pressure in the equations of incompressible fluid mechanics is necessary to impose incompressibility. In the present problem, if $p_{,\theta}$ is set to zero arbitrarily, there is a conflict because one has the two Eqs. (18) and (19) for one unknown function [$g(\cdot)$ here]. Neglecting the pressure term is also unphysical because this pressure depends on θ in such a way that it tends to different values as θ tends to π and $-\pi$. This nonzero pressure difference yields the

lift force on the semi-infinite plate that is the integral along the surface of the plate of the pressure difference given by the following expression:

$$p_t(\pi) - p_t(-\pi) = \int_{-\pi}^{\pi} d\theta \; (p_t)_{,\theta}. \tag{26}$$

where $(p_t)_{,\theta}$ is given by Eq. (25). Furthermore, this pressure difference is also needed to balance the loss of energy in the turbulent mixing layer.

B. Stress tensor $\tilde{\sigma}_{ij}$

As defined in Eq. (3), the stress tensor $\tilde{\sigma}_{ij}$ depends (linearly) on the rate of strain tensor τ_{ij} defined as

$$\tau_{ij} = U_{i,j} + U_{j,i}. \tag{27}$$

Introducing the stream function $\Psi = rg(\theta)$ in Eq. (27), the components of the strain tensor τ_{ij} become

$$\tau_{xx} = \frac{2}{r'} \sin\theta' \cos\theta' (g + g'') = -\tau_{yy}, \tag{28}$$

$$\tau_{xy} = \frac{\sin^2\theta' - \cos^2\theta'}{r'} (g + g''). \tag{29}$$

The relation $\tau_{yy} + \tau_{xx} = 0$ is a straight consequence of the incompressibility in two dimensions. As explained in the Introduction, it shows that the contribution $\tilde{\sigma}_{ij}$ to the stress tensor σ_{ij} does not meet the requirement of realizability by itself, because the trace of the Reynolds stress has to be positive, whereas the tensor $\tilde{\sigma}_{ij}$ has a vanishing trace. Recall that the diagonal tensor $\sigma_{ij}^{\mathrm{Re},p}$ called turbulent pressure has been added to $\tilde{\sigma}_{ij}^{\mathrm{Re}}$ in Eq. (2) in order to correct this point.

To lighten the coming algebra, let us introduce a new tensor $\tilde{\tau}_{ij}$ defined by

$$\tau_{ij} = \frac{1}{r} \tilde{\tau}_{ij}(\theta) \tag{30}$$

in order to split the integrals in Eqs. (3) and (4) into one involving the angle only, multiplied by another one involving r' which can be carried explicitly. The problem of writing explicitly the momentum balance is now reduced to an integral equation for θ-dependent functions only.

1. Momentum balance

Because the dependence on z and z' is only in the denominators of $(\frac{1}{|\mathbf{X}-\mathbf{X}'|} - \frac{1}{|\mathbf{X}'|})$, the integral over z' can be carried explicitly. Now concerning the integration over the variable r' in the definition of $\tilde{\sigma}_{ij}^{\mathrm{Re}}(\mathbf{X})$, the integral written in Eq. (3) reduces to $|(g+g'')(\theta')|^{\alpha} \tilde{\tau}_{ij}(\theta') \int_0^{\infty} dr' r'^{-\alpha} \ln(1 + (r/r')^2 - 2(r/r')\cos(\theta - \theta'))$, where $\tilde{\tau}$ is defined in Eq. (30). Setting $\zeta = r'/r$ allows to get rid of the variable r, and we get

$$\tilde{\sigma}_{ij}^{\mathrm{Re}}(\mathbf{X}) = \rho\, \tilde{\gamma} |(g+g'')|^{1-\alpha} \int d\theta' \, \tilde{\tau}_{ij}(\theta') \, |(g+g'')(\theta')|^{\alpha} \mathcal{I}(\theta - \theta'), \tag{31}$$

where the kernel $\mathcal{I}$ is defined by the relation

$$\mathcal{I}(\theta - \theta') = \int_0^{\infty} \frac{d\zeta}{\zeta^{\alpha}} \ln\left(\frac{1 + \zeta^2 - 2\zeta\cos(\theta - \theta')}{\zeta^2}\right). \tag{32}$$

This integral converges if $0 < \alpha < 1$ as assumed. Integrating by parts one obtains

$$\mathcal{I}(\theta - \theta') = \frac{2}{1-\alpha} \int_0^{\infty} \frac{\zeta^{-\alpha} d\zeta}{1 + \zeta^2 - 2\zeta\cos(\theta - \theta')} (1 - \zeta\cos(\theta - \theta')). \tag{33}$$

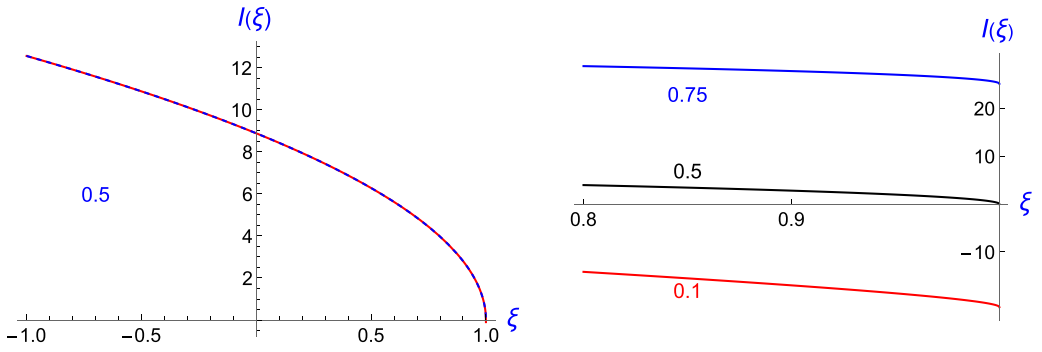

FIG. 2. (a) Functions $\hat{\mathcal{I}}(\xi)$ versus $\xi = \cos(\theta - \theta')$ for $\alpha = 1/2$; the numerical curve (solid line) is very well fitted by $8.88577\sqrt{1-\xi}$ (dashed line). (b) Behavior of $\hat{\mathcal{I}}(\xi)$ versus $\xi = \cos(\theta - \theta')$ for small values of $\theta - \theta'$, and various values of the exponent α written explicitly close to the curves. In the full domain $-1 \leqslant \xi \leqslant 0$ the coefficients in Eq. (36) are $a = -21.5$, $b = 9.3$, and $c = 16$ for $\alpha = 1/10$, and for $\alpha = 3/4$ the coefficients are $a = 25.2$, $b = 8.4$, and $c = -0.8$.

The equation to be satisfied by $g(\cdot)$ will be deduced by putting all the above results into Eq. (24). Consider first the contribution of the term of inertia, namely, the tensor $U_i U_j$ when dropping the factor ρ. Defining by C its contribution to the left-hand side of Eq. (24), which can be written as a quantity quadratic with respect to g and its derivatives, we get the simple looking result

$$C = -g(g + g'') \tag{34}$$

(see Appendix A for details). Let us call D the other contribution to the left-hand side of Eq. (24) which comes from the turbulent stress. Using the expressions given above, one obtains

$$D = -\tilde{\gamma}\frac{d}{d\theta}\left(|(g+g'')(\theta)|^{1-\alpha}\int_{-\pi}^{\pi} d\theta' \mathcal{I}(\theta-\theta')\right)|(g+g'')(\theta')|^{\alpha}(g+g'')(\theta')\cos 2(\theta-\theta') \tag{35}$$

as detailed in Appendix B. The integral over θ' is carried over the full angle, namely, from $-\pi$ to π, even though the mixing layer is expected to be concentrated near $\theta = 0$. However, we assume that the perturbation to the incoming potential flow, which extends itself to the full angular domain, has a very small amplitude far from the angular wedge of the mixing layer. This view is confirmed by the calculation done in Sec. III in the limit of a small velocity difference between the two sides of the mixing layer, and by experiments. Looking at the literature it is not obvious to see if a strictly bounded turbulent wedge is predicted, which poses the problem of the condition across the limit of this region or if a smooth continuity exists between the potential flow and the turbulent layer. Practically the matter is not that meaningful since a turbulent domain penetrating into the potential flow with an exponentially decaying amplitude does not make much difference with an exactly bounded nonpotential domain.

Setting $\xi = \cos(\theta - \theta')$ and $\hat{\mathcal{I}}(\xi) = \mathcal{I}(\theta - \theta')$, we observe (see Fig. 2) that the function $\hat{\mathcal{I}}(\xi)$ is very well fitted by a low-order polynomial in powers of $\sqrt{1-\xi}$,

$$\hat{\mathcal{I}}(\xi) = a_\alpha + b_\alpha\sqrt{1-\xi} + c_\alpha(1-\xi) \tag{36}$$

or $\mathcal{I}(\theta - \theta') = a_\alpha + b_\alpha|\theta - \theta'| + \cdots$, where the numerical coefficients $a_\alpha, b_\alpha, \ldots$ depend on the exponent α (see Fig. 2 caption). The curves in Fig. 2(b) display the behavior of $\hat{\mathcal{I}}(\xi)$ for ξ close to unity, namely, for small values of $\theta - \theta'$, and for three different values of α.

The problem of computing the average properties of the turbulent mixing layer has been reduced to the search of solutions of the equation

$$C + D = 0, \tag{37}$$

where C and D, given by Eqs. (34) and (35), are functions of $g(\theta)$ and its derivatives. Those equations have an interesting and nontrivial structure reflecting the fundamental principles from which they have been derived. Of course they do not at all include explicit dependence on quantities like a length or a time. Moreover, they are both quadratic with respect to $g(\cdot)$, as a consequence of the fact that no velocity scale should be introduced, besides the one arising from the average velocity itself. Equation (37) has an obvious solution $g = -U\sin(\theta - \theta_0)$ with arbitrary constants U and θ_0, coming from

$$g + g'' = 0. \tag{38}$$

However, this solution corresponds to a uniform velocity of strength U in a direction depending on the arbitrary angle θ_0 that does not correspond to the case of the mixing layer treated here. The problem of the mixing layer corresponds to a solution of Eq. (37) with a boundary condition for $g(\theta)$ deduced from the condition that u tends to U_1 and U_2 respectively as θ tends to $\pm\pi$ ($U_{1,2}$ being the incident velocities above and below the board; see Fig. 1), and v tends to zero because the incident flow is parallel to the board. Were those two values $U_{1,2}$ the same, the solution is just $g = -U\sin\theta$, namely, a uniform flow on both sides of the splitter. Below we look at the case where the two different values U_1 and U_2 are close to each other. Because of the nonlinear character of Eq. (37), this makes already a nontrivial question.

2. Pressure difference on the two sides of the plate

Let us return to the general relation (26) for the difference of pressure between the upper and lower parts of the plate. Equation (14) without the pressure term is

$$\tilde{\Sigma}_{ij} = \rho\, U_i U_j + \tilde{\sigma}_{ij}^{\mathrm{Re}}(\mathbf{X}). \tag{39}$$

We show in Appendix C that the derivative of the pressure with respect to the angle θ is given by the integral

$$(p_t)_{,\theta}(\theta) = -\rho\,\tilde{\gamma}\int_{-\pi}^{\pi} d\theta' \frac{d}{d\theta}\Big(|(g+g'')(\theta)|^{1-\alpha} d\theta' \mathcal{I}(\theta-\theta')\Big)|(g+g'')(\theta')|^{\alpha}\sin 2(\theta-\theta'). \tag{40}$$

Looking at the definition of $\tilde{\Sigma}_{ij}$ in Eq. (39), we emphasize that the gradient of the total pressure is caused by the effect of the stress tensor, $\tilde{\sigma}_{ij}^{\mathrm{Re}}$, since the first term U_iU_j yields a null contribution to relation (25) leading to the expression of $(p_t)_{,\theta}$ in Eq. (40). Integrating by parts Eq. (40), we get the following relation for the pressure difference between the two sides of the board:

$$\begin{aligned} p_t(\pi) - p_t(-\pi) = 2\rho\,\tilde{\gamma}\iint_{-\pi}^{\pi} d\theta\, d\theta' |(g+g'')(\theta)|^{1-\alpha}\mathcal{I}(\theta-\theta') \\ \times |(g+g'')(\theta')|^{\alpha}\,(g+g'')(\theta')\cos 4(\theta-\theta'). \end{aligned} \tag{41}$$

III. LIMIT OF SMALL VELOCITY DIFFERENCE

A. Scaling law between $\delta\theta$ and η

From the way the turbulent mixing layer is described, there is one dimensionless number in the data, the relative velocity difference

$$\eta = \frac{U_1 - U_2}{U_1 + U_2}. \tag{42}$$

Therefore, besides scaling parameters like the mean velocity $U = (U_1 + U_2)/2$, every observable quantity of the mixing layer depends on the ratio $\frac{U_1-U_2}{U_1+U_2}$, especially the angle $\delta\theta$ of the turbulent wedge. The relation between the angle $\delta\theta$ and the dimensionless velocity difference η is the most obvious function to be investigated. It would be used to test theories.

After looking at various possibilities for the relationship between η and $\delta\theta$ in the limit where both quantities are small, we found only one way to derive such a relation. It is based upon the fact that the balance of stress depends on the unknown function $g(\theta)$ only. Moreover, g appears both in C and in D through the combination $(g + g'')$, except for the prefactor g in C which is crucial for finding the relation between $\delta\theta$ and η. All the analysis relies on the behavior of u, v, and g for small values of the two small parameters $\delta\theta$ and η.

In the present section we derive an estimate of the scaling relation between $\delta\theta$ and η, leaving the quantitative study to the next section. Let us expand the functions u, v, and g in powers of η in the form $f(\theta) = f^{(0)} + \eta f_1 + \cdots$.

Assume first that $\eta = 0$ which is the case of a uniform velocity flow incident on the board in the x direction. In this case there is no turbulent flow behind the board. It follows that the zero-order solution is

$$\begin{cases} u^{(0)} = U \qquad \text{and} \qquad v^{(0)} = 0 \\ g^{(0)}(\theta) = -U \sin\theta, \qquad (g + g'')^{(0)} = 0. \end{cases} \tag{43}$$

For small θ the approximation $g^{(0)} \approx -U\theta$ has to be used with caution because we deal with expressions having derivatives with respect to θ which are expected to change rapidly in a small interval of width $\delta\theta$. This fast dependence is linked to the need to extrapolate the velocity field, from its value U_1 on one side of the mixing layer to U_2 on the other side. The corresponding correction to $u(\cdot)$ of order η is

$$u(\theta) = U(1 + \eta u_1(\theta)) + \cdots, \tag{44}$$

where u_1 is of order unity because the velocity $u(\theta)$ is equal to U for $\theta = 0$ and equal to $U(1 \pm \eta)$ for $\theta = \pm\pi$. Similarly we can set

$$g = g^{(0)} + \eta g_1, \tag{45}$$

having in mind that g_1 is not necessarily of order unity, because the terms g_1 and g_1' are linked to u_1 by the relation

$$g_1 \sin\theta + g_1' \cos\theta = -U u_1. \tag{46}$$

Equation (46) can be approximated by taking into account the small angular spreading $\delta\theta$ of the mixing layer which makes the successive derivatives of g_1 bigger and bigger; more precisely we have $g_1' \sim g_1/\delta\theta$, $g_1'' \sim g_1/(\delta\theta)^2$. Therefore, Eq. (46) gives $g_1' \sim U$, or

$$g_1 \sim U\delta\theta, \tag{47}$$

which proves that g_1 is not of order unity, as announced above. In summary at first order with respect to η one has $(g + g'')_{(1)} \approx \eta g_1'' \sim \eta g_1/(\delta\theta)^2$ which becomes $(g + g'')_{(1)} \sim U/\delta\theta$ when using relation (47), or

$$(g + g'') \sim \eta U/\delta\theta. \tag{48}$$

Taking this order of magnitude for $(g + g'')$ in D, giving to θ the order of magnitude $\delta\theta$, and assuming that $\mathcal{I}(\theta - \theta')$ is constant in the small wedge, and nonzero, one can estimate $D \sim (g'')^2$. Consider now C, which has the magnitude $g(g + g'') \sim g^{(0)}(g + g'')$. The relation $C + D = 0$ leads naturally to the constraint that, if C and D are of the same order of magnitude, then $g^{(0)} \sim g''$ or using Eqs. (43) and (48),

$$\delta\theta \sim \eta^{1/2}. \tag{49}$$

Note that in the peculiar case of the exponent $\alpha = 1/2$ (and close to this value), discussed in Appendix D, the above scaling is not valid because $\mathcal{I}(0) = 0$ as shown in Fig. 2(a). Instead of this approximation, we have to consider the solution $\mathcal{I}(\theta - \theta') = b|(\theta - \theta')|$ written in the caption of this figure, which is of order $b\delta\theta$. In that case the condition $C + D$ leads to the linear relation

$$\delta\theta \sim \eta \qquad \text{for} \qquad \alpha = 1/2. \tag{50}$$

The estimate in Eq. (49) is interesting because it shows a kind of amplification of the fluctuations, at least in this small-η limit. As far as the order of magnitude is concerned, η can be seen as a dimensionless measurement of the given velocity difference driving the instability. It is quite natural to compare it to the amplitude of the velocity fluctuations taking place inside the turbulent wedge. As shown in Sec. III B 2, the variance of the velocity fluctuations $\langle u'^2 \rangle$ is of order $\eta^{3/2}U^2$ [see Eq. (63)], which is much larger (as η tends zero) than the square of velocity difference across the mixing layer, $(U_1 - U_2)^2$, of order $\eta^2 U^2$.

Another point of interest is the extension of the estimate of the angular width of the turbulent wedge to other situations. We already noticed that such wedges should appear when a parallel flow hits a half plane making a nonzero angle with the flow direction. Applying the same idea as above to this situation one can find the order of magnitude of the angle of the turbulent wedge in the limit of large Reynolds number. In this limit the perturbation (similar to η above) brought by the half plane is the angle β of the half plane with respect of the incoming flow. Let us assume that this angle is small. Because it enters in the boundary conditions in the equations for the function $g(\theta)$ like the boundary condition on the two sides of the splitter plate, we could conjecture that the relationship between β and $\delta\theta$ displays the same power law as the one between β and $\delta\theta$, namely,

$$\delta\theta \sim \beta^{1/2}, \tag{51}$$

which also involves geometrical quantities only.

B. Solution for small η and $\delta\theta$

Here we go further than scaling relations, by deriving the solution for the time-averaged velocity field for small values of η and $\delta\theta$, that allows to give to Eq. (49) a quantitative expression. As usual in this kind of analysis, once the relationship between the various quantities is found, one can get a parameterless equation to be satisfied by the unknown function. In the present case it amounts to finding the equation for u_1 and g_1 defined in Eqs. (44) and (46) as a function of the angle

$$\tilde{\theta} = \theta/\delta\theta, \tag{52}$$

where $\delta\theta$ is positive, linked to η, and should agree ultimately with relation (49). In the final stage of our derivation the small angle $\delta\theta$ will be defined as the half width at half height of the velocity derivative $u'(\theta)$ (see Fig. 4 in Appendix D). In order to handle functions of $\tilde{\theta}$ which are of order unity, we define $\tilde{g}_1(\tilde{\theta})$ and its derivative with respect to $\tilde{\theta}$ by the relations

$$g_1(\theta) = U\delta\theta\, \tilde{g}_1(\tilde{\theta}), \qquad g_1'(\theta) = U\tilde{g}_1'(\tilde{\theta}), \qquad g_1''(\theta) = \frac{U}{\delta\theta}\tilde{g}_1''(\tilde{\theta}). \tag{53}$$

The derivation of the solution of the equation for $g_1''(\theta)$ is detailed in Appendix D. This equation for $g_1''(\theta)$ is deduced from $C + D = 0$ written in terms of the tilde quantities which becomes

$$\tilde{\theta}\tilde{g}_1'' = \tilde{\gamma}\mathcal{I}(0)\tilde{\mathcal{J}}\frac{1-\alpha}{\alpha}|\tilde{g}_1''(\tilde{\theta})|^{-\alpha}\frac{d}{d\tilde{\theta}}|\tilde{g}_1''(\tilde{\theta})|. \tag{54}$$

The solution of Eq. (54) is of the form

$$|\tilde{g}_1''(\tilde{\theta})| = G_0\left(1 + (\frac{\tilde{\theta}}{\tilde{\theta}_c})^2\right)^{-1/\alpha}, \tag{55}$$

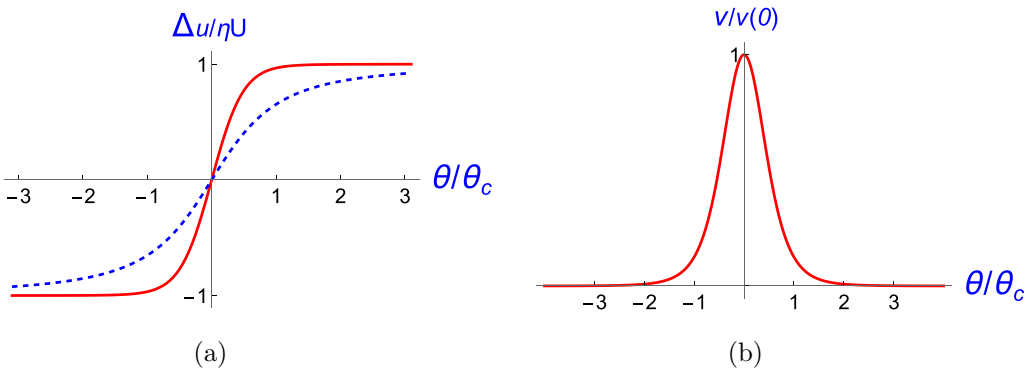

(a) (b)

FIG. 3. (a) Profile of the x component of the velocity versus θ/θ_c, Eq. (57), for two values of the exponent, $\alpha = 0.25$ for the solid red line, $\alpha = 0.75$ for the dashed blue line. The increment $\Delta u = u - U$ is scaled to $\eta U = (U_1 - U_2)/2$ and the polar angle θ is scaled to $\theta_c = \delta\theta\ \tilde{\theta}_c$ with $\tilde{\theta}_c$ given in Eq. (D20). The asymptotic values of u are U_1 (respectively U_2) as θ tends to $\pm\infty$. (b) Profile of the y component of the velocity, Eq. (58) versus θ/θ_c for $\alpha = 0.25$; v is scaled to $v(0) = -(1/2)\eta^{3/2}k^{1/2}(U/d_\alpha)\alpha/(1-\alpha)$.

where $\tilde{\theta}_c$ is a number which depends on the value of the exponent α [see Eq. (D25)], and $G_0 = -\tilde{g}_1''(0)$ is positive and depends on the solution itself. Indeed we point out that in order to solve Eq. (54) one has to solve the bootstrap condition that $\tilde{\mathcal{J}}$ is given by the value figuring in the solution, and to take into account the behavior of the solution at the boundaries. This procedure allows to get the following quantitative relation between the two small parameters $\delta\theta$ and η:

$$\delta\theta^2 = \eta\left(\tilde{\gamma}\mathcal{I}(0)\,\frac{4}{\tilde{\theta}_c^2}\,\frac{1-\alpha}{\alpha}\,\frac{c_\alpha}{d_\alpha}\right), \tag{56}$$

where all coefficients in the parentheses, $\tilde{\theta}_c$, c_α, d_α, and $\mathcal{I}(0)$, are numerical ones and dimensionless. The coefficient $\tilde{\gamma}$ has to be of opposite sign with respect to $\mathcal{I}(0)$, so it must be negative for $\alpha < 1/2$ and positive for $\alpha > 1/2$ [see Fig. 5(a), plotting $\mathcal{I}(0)$ versus α]. Note that besides this constraint, the exponent α and coefficients $\tilde{\gamma}$ in front of the integral defining $\tilde{\sigma}_{ij}^{\mathrm{Re}}$ remain arbitrary and so need to be fitted with experiments.

Unfortunately, few experiments have been made in the regime of small η, namely, with two incident flows of quasiequal velocities $U_1 \approx U_2$. Nevertheless, we found an experimental study extending from $\eta = 0.05$ up to $\eta = 0.6$ [12], with many references to other works. In Table 3.2 of Ref. [12] the author compares his measurement of the turbulent wedge angle versus η with other measurements. Only two experiments cover the range of small η values, the one of the author and

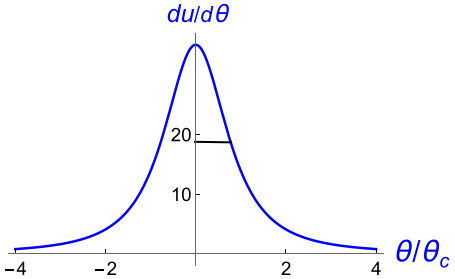

FIG. 4. Derivative of the velocity component, $u_{,\theta}$ versus θ/θ_c, for $\eta = 0.26$, $\alpha = 3/4$. The half width at half height is indicated by the segment $\delta\theta = 0.02$ (data of Ref. [12]) and Eq. (D20) yields $\theta_c = 0.025$.

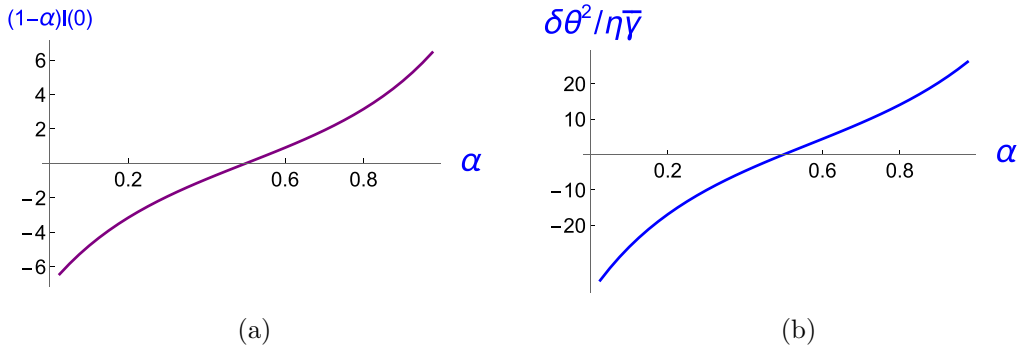

(a) (b)

FIG. 5. (a) $(1-\alpha)\mathcal{I}(0)$ versus α [see Eq. (D27)]. (b) Ratio $\delta\theta^2/\eta\tilde{\gamma}$ versus α given in Eq. (56). The product $\tilde{\gamma}\mathcal{I}(0)$ has to be positive; then $\tilde{\gamma} < 0$ for $\alpha < 1/2$.

the one of Mehta [13]. In this domain both curves $\delta\theta$ versus η, display similar nonlinear behavior [see Fig. 6(a)]. As detailed in Appendix E, in the range of small η, the two experiments agree with the relation $\delta\theta \sim \eta^{1/2}$ plotted in Fig. 6(b).

Let us recall that this scaling law was predicted (in the frame of our model) in the limit of small η, and for $\alpha \neq 1/2$, more precisely for $\mathcal{I}(0)$ much larger than $b_\alpha\delta\theta$ [see Eq. (36)], that would give possible α values either close to unity, or close to zero. Moreover, from the curve in Fig. 6(b), one may deduce the value of the ratio $\delta\theta/\eta^{1/2}$ that allows to fix the value of the free parameter $\tilde{\gamma}$ [see Eq. (E1)], which depends on α as illustrated in Fig. 7.

Finally the profile of the longitudinal and transverse velocity components, deduced from solution (55), are given by the expressions

$$u(\theta) - U = \frac{\eta U}{d_\alpha}\int_0^{\theta/\theta_c} dy\,(1+y^2)^{-1/\alpha}, \tag{57}$$

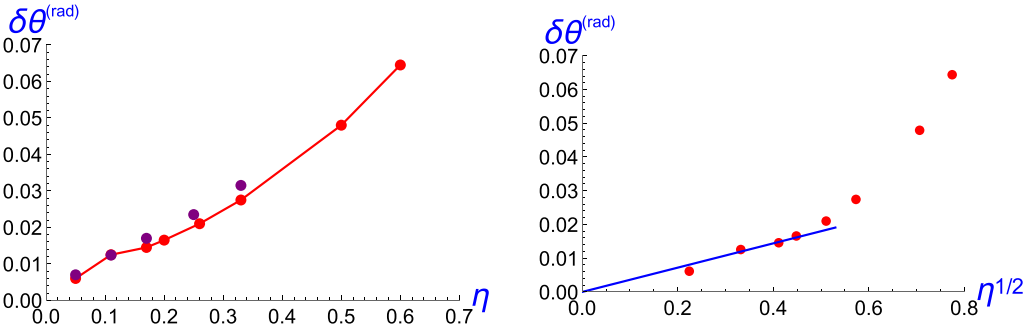

(a) (b)

FIG. 6. Angular width $\delta\theta$ from experimental data summarized in Table 3.2 of Ref. [12]: (a) Half angle of the turbulent domain as a function of η and (b) same measure as a function of $\eta^{1/2}$. In (a) the red points on the solid line correspond to measurements made by the author of Ref. [12]. Their behavior surprisingly agrees with that of data deduced from Ref. [13] (purple points, with ordinate enhanced by a factor of 2 for comparison). In (b) the data reasonably agree with the prediction of our model, $\delta\theta \sim \eta^{1/2}$ for small values of η and even medium values. The blue line of (b) is drawn to compare experimental points with our prediction.

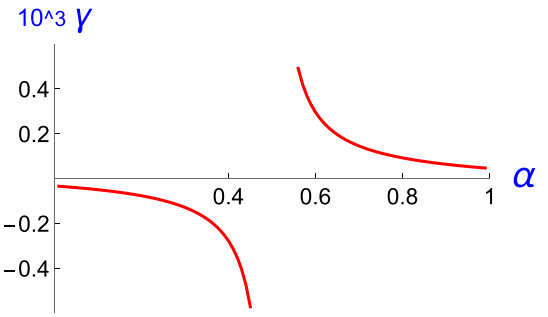

FIG. 7. $10^3\tilde{\gamma}$ versus the exponent α. The numerical value of the prefactor $\tilde{\gamma}$ is deduced from the data of Ref. [12] and from relation (E1). Recall that in a domain close to $\alpha = 1/2$, the approximation $\mathcal{I}(\theta - \theta') \approx \mathcal{I}(0)$ is not valid because $\mathcal{I}(0) = 0$ [see Fig. 2(a)].

where d_α is the value of the integral for $\theta/\theta_c = \infty$, given in Eq. (D23), and

$$v(\theta) = -\frac{\eta^{3/2} U k^{1/2} \tilde{\theta}_c}{d_\alpha} \frac{\alpha}{2(1-\alpha)} \left(1 + \frac{\theta^2}{\theta_c^2}\right)^{-\frac{1-\alpha}{\alpha}}, \tag{58}$$

where $\theta_c = \tilde{\theta}_c \delta\theta$ and $k = \delta\theta^2/\eta$ is a constant deduced from Eq. (56),

$$k = \tilde{\gamma}\mathcal{I}(0) \frac{4}{\tilde{\theta}_c^2} \frac{1-\alpha}{\alpha} \frac{c_\alpha}{d_\alpha}, \tag{59}$$

which is positive because the product $\tilde{\gamma}\mathcal{I}(0)$ must be positive. The profiles are drawn in Fig. 3. In Fig. 3(a) the role of the exponent α appears artificially because of the scaled abscissa, although the two curves have the same half width $\delta\theta$ by definition.

Let us notice that the solution found above for the velocity field is a solution of the third-order ordinary differential equation (37) deduced from the model of Eqs. (3) and (4), although the velocity field satisfies four boundary conditions ($u - U = \pm\eta U$ and $v = 0$ on the slider sides). This was possible because of the symmetry of the solution for small η values. But it could happen that for η of order unity, one has to modify Eqs. (3) and (4) by including a kernel satisfying Eq. (5), as written in the Introduction, a problem not treated here.

1. Pressure difference on the plates

Let us finally consider the order of magnitude of the pressure difference between the two plates. As shown in Appendix C, we get

$$p(\pi) - p(-\pi) \sim (\eta U)^2. \tag{60}$$

Therefore, the difference of pressure reflects the lift force which is quadratic with respect to $(U_2 - U_1)$, as expected.

2. Order of magnitude of $\tilde{\sigma}_{ij}^{\mathrm{Re}}$ and $\sigma_{ii}^{\mathrm{Re},p}$

As detailed in the Appendix F, the orders of magnitude of the components of $\tilde{\sigma}_{ij}^{\mathrm{Re}}$ are

$$\begin{cases} \tilde{\sigma}_{xx}^{\mathrm{Re}} = -\tilde{\sigma}_{yy}^{\mathrm{Re}} \sim \eta^{5/2} \\ \tilde{\sigma}_{xy}^{\mathrm{Re}} \sim \eta^{3/2}. \end{cases} \tag{61}$$

As expected these relations do not satisfy the realizability conditions (F7), because one diagonal component is negative; moreover, $\sigma_{xy}^2 > \sigma_{xx}\,\sigma_{yy}$ which is invalid for correlation functions.

Let us now consider the order of magnitude of the diagonal elements of the tensor $\sigma_{ij}^{\mathrm{Re},p}$ defined in Eq. (4). In the mixing layer case they become

$$\sigma_{ii}^{\mathrm{Re},p}(\theta) = \rho\,\tilde{\gamma}\,|(g+g'')|^{1-\alpha}\int d\theta' \mathcal{I}(\theta-\theta')|(g+g'')(\theta')|^{\alpha}(g+g'')(\theta'). \tag{62}$$

They are of order $(g'')^2$ times $\delta\theta$ (which comes from the integration), which gives

$$\sigma_{ii}^{(\mathrm{Re},p)} \sim \eta^{3/2}, \tag{63}$$

which is of the same order as $\tilde{\sigma}_{xy}^{\mathrm{Re}}$. Therefore, the realizability conditions (F7) can be fulfilled by the sum of the two tensors in Eq. (1). Moreover, the off-diagonal element $\tilde{\sigma}_{xy}^{\mathrm{Re}}$ contains an integrand smaller than the diagonal one $\sigma_{ii}^{(\mathrm{Re},p)}$ because of the presence of $\cos 2(\theta-\theta')$ in $\tilde{\sigma}_{xy}^{\mathrm{Re}}$, compared to unity in $\sigma_{ii}^{(\mathrm{Re},p)}$. It follows that the realizability conditions are fulfilled by taking the same constant for the two tensors in Eqs. (3) and (4), namely, $\gamma = \tilde{\gamma}$, that correspond to on-axis fluctuations $\langle u'v'\rangle$, $\langle u'^2\rangle$, and $\langle v'^2\rangle$ of quasiequal amplitude for small η within the frame of our model. However, the ratio $\gamma/\tilde{\gamma}$ has to be adjusted with experimental results, which could give a value larger than unity, although we have not found any profile of velocity fluctuations for small values of η, most of them being concerned about ratios U_1/U_2 of order of a few units.

In summary, starting with a model including three free parameters, α, $\tilde{\gamma}$, and γ, we have been able to specify that the exponent α is different from $1/2$ and to deduce the value of the two factors $\tilde{\gamma} \approx \gamma$ from the experimental slope of $\delta\theta/\eta^{1/2}$.

IV. CONCLUSIONS AND PERSPECTIVES

In this paper we wrote fully explicitly the integral equation for the balance of momentum including the closure of the turbulent stress introduced in Ref. [4] on the basic assumption that dissipation is caused by singular events described by solutions of Euler's equation.

Notice that this fully explicit closure yields equations with all the expected scaling laws, which is not surprising because the equations are derived to this end. In addition we emphasize that quantitative properties can be put in evidence, including the effect of boundary conditions. This point is nontrivial because the boundary conditions make often a nontrivial issue for integral equations.

Our detailed analysis, applied to the turbulence behind the plate in the mixing layer setup, is performed in the limit of a small velocity difference η. In this limit we have found only few experiments reported; nevertheless, they agree with our prediction that the angular spreading of the turbulent domain $\delta\theta$ scales as $\eta^{1/2}$ for any values of the exponent α (except $\alpha \approx 1/2$ leading to $\delta\theta \sim \eta$). From this agreement one is able to extract the value of one of the three free parameters α, $\tilde{\gamma}$, and γ of our model. The more general case of η of order unity is in progress. We hope it would yield a deeper comparison between our model and numerical or experimental data. In particular this would allow to give the value, even approximate, of the exponent α.

Of course one can also hope to get solutions of the momentum balance in situations more complex than the one considered here. We think first to an axisymmetric wake like the one behind a disk perpendicular to the incoming flow. In this case one has to consider two variables, the position in the flow direction and the radius in the perpendicular direction, although the mixing layer study deals with a single variable (the angle, which is the ratio of these two variables) , but the question of imposing the boundary condition is nontrivial. We plan to study those flows in the near future.

ACKNOWLEDGMENT

We greatly acknowledge Christophe Josserand and Sergio Rica for fruitful and stimulating discussions.

APPENDIX A: CONTRIBUTION OF THE INERTIA TO EQ. (24)

Here we derive Eq. (34) which represents the contribution of the inertia to Eq. (24). We have to insert in Eq. (24) the first term U_iU_j of the tensor

$$\tilde{\Sigma} = U_iU_j + \tilde{\sigma}_{ij}^{\mathrm{Re}}. \tag{A1}$$

With $U_x = u$ and $U_y = v$, we get

$$C = \sin\theta\cos\theta\left((v^2)_{,\theta} - (u^2)_{,\theta}\right) + (\cos^2\theta - \sin^2\theta)(uv_{,\theta} + vu_{,\theta}). \tag{A2}$$

By definition of (u, v) in polar coordinates,

$$\begin{cases} u(\theta) = -(g\sin\theta + g'\cos\theta) \\ v(\theta) = g\cos\theta - g'\sin\theta, \end{cases} \tag{A3}$$

we have

$$\begin{cases} u_{,\theta} = -(g + g'')\cos\theta \\ v_{,\theta} = -(g + g'')\sin\theta. \end{cases} \tag{A4}$$

Inserting these derivatives in Eq. (A2) we obtain

$$\frac{C}{g + g''} = \sin 2\theta(-g\sin 2\theta - g'\cos 2\theta) + \cos 2\theta(-g\cos 2\theta + g'\sin 2\theta), \tag{A5}$$

which reduces to

$$\frac{C}{g + g''} = -g, \tag{A6}$$

or Eq. (34).

APPENDIX B: CONTRIBUTION OF THE STRESS TENSOR $\tilde{\sigma}_{ij}^{\mathrm{Re}}$ TO EQ. (24)

Here we derive Eq. (35) which represents the contribution of the nondiagonal Reynolds stress tensor $\tilde{\sigma}_{ij}^{\mathrm{Re}}$ to Eq. (24). We have to insert in Eq. (24) the second term of the tensor $\tilde{\Sigma}$ defined in Eq. (A1), which gives

$$D = \frac{1}{2}\sin 2\theta(\tilde{\sigma}_{yy}^{\mathrm{Re}} - \tilde{\sigma}_{xx}^{\mathrm{Re}})_{,\theta} + \cos 2\theta(\tilde{\sigma}_{xy}^{\mathrm{Re}})_{,\theta}. \tag{B1}$$

Using Eq. (30) and Eqs. (28) and (29), the components of $\tilde{\tau}_{ij}$ become

$$\begin{cases} \tilde{\tau}_{xx} = \sin 2\theta(g + g'') = -\tilde{\tau}_{yy} \\ \tilde{\tau}_{xy} = -\cos 2\theta(g + g'') = \tilde{\tau}_{yx}. \end{cases} \tag{B2}$$

Inserting these latter expressions in the integrand of Eq. (31), we get

$$D = B_1\sin 2\theta + B_2\cos 2\theta, \tag{B3}$$

where

$$B_1 = -\tilde{\gamma}\frac{d}{d\theta}\left(|(g + g'')(\theta)|^{1-\alpha}\int_{-\pi}^{\pi} d\theta'\mathcal{I}(\theta - \theta')\right)|(g + g'')(\theta')|^{\alpha}\,(g + g'')(\theta')\,\sin 2\theta' \tag{B4}$$

and

$$B_2 = -\tilde{\gamma}\frac{d}{d\theta}\left(|(g + g'')(\theta)|^{1-\alpha}\int_{-\pi}^{\pi} d\theta'\mathcal{I}(\theta - \theta')\right)|(g + g'')(\theta')|^{\alpha}\,(g + g'')(\theta')\,\cos 2\theta'. \tag{B5}$$

Equations (B3)–(B5) are equivalent to the compact form of Eq. (35).

APPENDIX C: PRESSURE DIFFERENCE BETWEEN THE TWO SIDES OF THE PLATE

Here we derive expression (40) for the pressure gradient and the pressure difference (41) between the two sides of the plate. Looking at the equation

$$(p_t)_{,\theta} = -\sin^2\theta\ \tilde{\Sigma}_{xx,\theta} - \cos^2\theta\ \tilde{\Sigma}_{yy,\theta} + 2\sin\theta\cos\theta\ \tilde{\Sigma}_{xy,\theta} \tag{C1}$$

already written in Eq. (25), with $\tilde{\Sigma}$ defined in Eq. (A1), let us first consider the contribution of the inertia term U_iU_j to this expression for $p_{,\theta}$. This contribution is the sum $c_1 + c_2$ with

$$c_1 = -2uu_{,\theta}\sin^2\theta - 2vv_{,\theta}\cos^2\theta \tag{C2}$$

and

$$c_2 = 2(v\,u_{,\theta} + u\,v_{,\theta})\sin\theta\cos\theta. \tag{C3}$$

Using Eqs. (10), (11), and (A4), we get the relation

$$c_1/(g+g'') = g\sin 2\theta\cos 2\theta - g'(\sin 2\theta)^2 = -c_2/(g+g''), \tag{C4}$$

which shows that the inertia term does not contribute to the gradient of pressure in such two-dimensional (2D) geometry, as written in the text.

Consider now the effect of the tensor $\tilde{\sigma}_{ij}^{\mathrm{Re}}$, defined in Eq. (3). Separating, as above, the diagonal and nondiagonal terms of this tensor gives

$$(p_t)_{,\theta} = d_1 + d_2, \tag{C5}$$

with

$$d_1 = -(\tilde{\sigma}_{xx}^{\mathrm{Re}})_{,\theta}\sin^2\theta - (\tilde{\sigma}_{yy}^{\mathrm{Re}})_{,\theta}\cos^2\theta = \cos 2\theta(\tilde{\sigma}_{xx}^{\mathrm{Re}})_{,\theta} \tag{C6}$$

because $\tau_{xx} = -\tau_{yy}$, and

$$d_2 = \sin 2\theta(\tilde{\sigma}_{xy}^{\mathrm{Re}})_{,\theta}. \tag{C7}$$

Inserting in these relations Eqs. (28)–(30), we get

$$d_1 = \tilde{\gamma}\rho\cos 2\theta\frac{d}{d\theta}[|(g+g'')|^{1-\alpha}\int d\theta'\mathcal{I}(\theta-\theta')]\,|(g+g'')(\theta')|^{\alpha}(g+g'')(\theta')\sin(2\theta') \tag{C8}$$

and

$$d_2 = -\tilde{\gamma}\rho\sin 2\theta\frac{d}{d\theta}[|(g+g'')|^{1-\alpha}\int d\theta'\mathcal{I}(\theta-\theta')]\,|(g+g'')(\theta')|^{\alpha}(g+g'')(\theta')\cos(2\theta'). \tag{C9}$$

By integration of d_1 and d_2 over the variable θ running from $-\pi$ to $+\pi$, we obtain the presure difference on the plate. Integrating by parts the two terms in Eq. (C5), and taking into account the condition $g + g'' = 0$ at the boundary which allows to cancel the constant term of this integration (the term depending on the boundary values), we obtain

$$p_t(\pi) - p_t(-\pi) = 2\tilde{\gamma}\rho\iint_{-\pi}^{+\pi} d\theta'\,\theta'\cos 2(\theta-\theta')\,|(g+g'')(\theta)|^{1-\alpha}\mathcal{I}(\theta-\theta') \times |(g+g'')(\theta')|^{\alpha}(g+g'')(\theta'). \tag{C10}$$

From this expression we can derive the difference of pressure on the two sides of the plate in the limit of small difference between the two incident velocities. Using the arguments developed in Sec. III, we have $(g+g'') \sim \eta U/\delta\theta$ in the turbulent domain of angular extension $\delta\theta$. It follows that the order of magnitude of the integrand in Eq. (C10) is of order $(\eta U/\delta\theta)^2$, which has to be multiplied by $(\delta\theta)^2$ to represent the order of magnitude of the pressure difference. We obtain

$$p_t(\pi) - p_t(-\pi) \sim (\eta U)^2. \tag{C11}$$

We find that the lift force is quadratic with respect to $(U_2 - U_1)$, as expected from the Kutta-Zhukovsky theorem.

APPENDIX D: DERIVATION OF THE VELOCITY PROFILE AND RATIO $\delta\theta^2/\eta$

Here we derive the solution of $C + D = 0$ for small values of the two parameters η and θ. Assuming that $\mathcal{I}(\theta - \theta') = \mathcal{I}(0)$ and $\cos(\theta - \theta') = 1$ in the integrand of Eq. (35) (see below for the justification), we have to solve

$$-g(\theta)(g + g'') = \tilde{\gamma}\mathcal{I}(0)\mathcal{J}\frac{d}{d\theta}|(g + g'')|^{1-\alpha}, \tag{D1}$$

where

$$\mathcal{I}(0) = \frac{2}{1-\alpha}\int_0^\infty d\zeta\,\frac{1}{\zeta^\alpha(1-\zeta)}, \tag{D2}$$

$$\mathcal{J} = \int_{-\infty}^{\infty} d\theta'(g + g'')(\theta')|(g + g'')(\theta')|^\alpha. \tag{D3}$$

In a second step, after having found the solution for $g + g''$, we have to integrate

$$\begin{cases} u'(\theta) = -(g + g'')\cos\theta \\ v'(\theta) = -(g + g'')\sin\theta \end{cases} \tag{D4}$$

together with the four boundary conditions

$$u(\pm\pi) = U(1 \pm \eta), \qquad v(\pm\pi) = 0. \tag{D5}$$

Solution for $g^{(0)} \approx -U\theta$

For $\eta = 0$, the velocity components are

$$u^{(0)} = U \qquad \text{and} \qquad v^{(0)} = 0 \tag{D6}$$

and the g function is

$$g^{(0)}(\theta) = -U\sin\theta \qquad \text{or} \qquad (g + g'')^{(0)} = 0. \tag{D7}$$

Using these expressions for the leading-order solution we have to expand all functions in powers of η and θ, which will allow to get finally a scaling relation between the two small parameters θ and η. Let us define the dimensionless parameter

$$\tilde{\theta} = \theta/\delta\theta, \tag{D8}$$

where $\delta\theta$ (a positive quantity) is the small angular aperture of the turbulent domain. More precisely $\delta\theta$ will be defined below as the half width at half height of the velocity derivative $u'(\theta)$ (see Fig. 4). We can use relations (47) and (48) to define functions of $\tilde{\theta}$ which are of order unity. We set

$$g_1(\theta) = U\delta\theta\ \tilde{g}_1(\tilde{\theta}), \tag{D9}$$

which leads to

$$g_1'(\theta) = U\tilde{g}_1'(\tilde{\theta}), \qquad g_1''(\theta) = \frac{U}{\delta\theta}\tilde{g}_1''(\tilde{\theta}), \tag{D10}$$

where $\tilde{g}_1', \tilde{g}_1''$ are the derivatives of $\tilde{g}_1$ with respect to the variable $\tilde{\theta}$. Using the rescaling in (D8), the boundaries in the integral defining D are set to plus and minus infinity. In terms of the tilde quantities, the left-hand side of Eq. (D1) is

$$C/\rho = -\eta U^2\tilde{\theta}\,\tilde{g}_1''(\tilde{\theta}). \tag{D11}$$

The right-hand side,

$$-D/\rho = \tilde{\gamma}\mathcal{I}(0)\eta^2 \frac{d}{d\theta}\left(|g_1''(\theta)|^{1-\alpha}\right) \int_{-\infty}^{\infty} d\theta' g_1''(\theta')|g_1''(\theta')|^{\alpha}, \tag{D12}$$

becomes in tilde variables

$$-D/\rho = \tilde{\gamma}\mathcal{I}(0)(1-\alpha)\left(\frac{U\eta}{\delta\theta}\right)^2 \tilde{\mathcal{J}}\,|\tilde{g}_1''(\tilde{\theta})|^{-\alpha}\frac{d}{d\tilde{\theta}}|\tilde{g}_1''(\tilde{\theta})|, \tag{D13}$$

where we introduced

$$\tilde{\mathcal{J}} = \int_{-\infty}^{\infty} d\tilde{\theta}'\tilde{g}_1''(\tilde{\theta}')|\tilde{g}_1''(\tilde{\theta}')|^{\alpha}. \tag{D14}$$

In these expressions the sign of g_1'' is known because one has

$$u'(\theta) = -\eta\frac{U}{\delta\theta}\tilde{g}_1'' \tag{D15}$$

and we expect that the slope of the velocity profile $u(\theta)$ is positive for $\eta > 0$ (the case schematized in Fig. 1) and negative for $\eta < 0$, which imposes $\tilde{g}_1''(\tilde{\theta}) < 0$ in both cases. Setting $\tilde{g}_1''(\tilde{\theta}) = -|\tilde{g}_1''(\tilde{\theta})|$, and $\tilde{\mathcal{J}} = -|\tilde{\mathcal{J}}|$, Eq. (D1) becomes

$$\tilde{\theta} = \frac{\eta}{\delta\theta^2}\frac{1-\alpha}{\alpha}\tilde{\gamma}|\tilde{\mathcal{J}}|\mathcal{I}(0)\frac{d}{d\tilde{\theta}}|\tilde{g}_1''(\tilde{\theta}))|^{-\alpha}. \tag{D16}$$

By integration we obtain

$$|\tilde{g}_1''(\tilde{\theta})| = G_0\left(1 + (\frac{\tilde{\theta}}{\tilde{\theta}_c})^2\right)^{-1/\alpha}, \tag{D17}$$

where $G_0 = -\tilde{g}_1''(0)$ is positive, and

$$\tilde{\theta}_c^2 = 2(\eta/\delta\theta^2)\,((1-\alpha)/\alpha)\,|\tilde{\gamma}\,\tilde{\mathcal{J}}\,\mathcal{I}(0)|\,G_0^{-\alpha}. \tag{D18}$$

Now we have to take into account that the solution (D17) for $\tilde{g}_1''$ has to be put in $\tilde{\mathcal{J}}$ defined in Eq. (D3). We get $|\tilde{\mathcal{J}}| = (2\tilde{\theta}_c G_0^{\alpha+1}\,c_\alpha)$ where

$$c_\alpha = \int_0^{\infty} dy\,(1+y^2)^{-(1+\alpha)/\alpha} = \sqrt{\pi}\frac{\Gamma(\frac{\alpha+1}{\alpha} - \frac{1}{2})}{2\Gamma(\frac{\alpha+1}{\alpha})}, \tag{D19}$$

and $\Gamma(\cdot)$ is the usual gamma function. Putting the latter relations in Eq. (D18) gives

$$\tilde{\theta}_c = 4\frac{\eta}{\delta\theta^2}\frac{1-\alpha}{\alpha}\tilde{\gamma}\mathcal{I}(0)G_0 c_\alpha. \tag{D20}$$

Equation (D20) implies that the product $\tilde{\gamma}\mathcal{I}(0)$ has to be positive; it follows that the factor $\tilde{\gamma}$ in front of $\tilde{\sigma}_{ij}^{\mathrm{Re}}$ must be positive when the exponent α is bigger than $1/2$, and negative in the opposite case.

Now we have to take into account the boundary conditions of the velocity field which can be written as

$$\int_0^{\infty} d\theta\, u'(\theta) = \eta U. \tag{D21}$$

Using Eq. (D15) this relation becomes

$$G_0 d_\alpha \tilde{\theta}_c = 1, \tag{D22}$$

where

$$d_\alpha = \int_0^{\infty} dy(1+y^2)^{-1/\alpha} = \sqrt{\pi}\frac{\Gamma(1/\alpha - 1/2)}{2\Gamma(1/\alpha)}. \tag{D23}$$

Finally, we point out that the width of the solution $g''(\theta) \propto u'(\theta)$ depends on the value of the exponent α. In order to take this dependence into account we can define the angular width of the turbulent wedge as the half width at half height of $u'(\theta)$ (see Fig. 4), which amounts to setting

$$u'(\delta\theta) = \frac{1}{2}u'(0). \tag{D24}$$

Putting this expression in solution (55) equivalent to $u'(\theta) = u'(0)(1+\theta^2/\theta_c^2)^{-1/\alpha}$, with $\theta_c = \delta\theta\,\tilde{\theta}_c$, we get

$$\tilde{\theta}_c^2 = \frac{1}{2^\alpha - 1}, \tag{D25}$$

which yields a quantitative expression for relation (49),

$$\delta\theta^2 = \eta\left(\tilde{\gamma}\mathcal{I}(0)\,\frac{4}{\tilde{\theta}_c^2}\,\frac{1-\alpha}{\alpha}\,\frac{c_\alpha}{d_\alpha}\right), \tag{D26}$$

where all coefficients in parentheses are numerical ones and dimensionless, θ_c, c_α, and d_α are defined just above, $\mathcal{I}(0)$ is deduced from Eq. (33),

$$\mathcal{I}(0) = \frac{2}{1-\alpha}\int_0^\infty d\zeta\,\frac{1}{\zeta^\alpha(1-\zeta)}, \tag{D27}$$

and the coefficient $\tilde{\gamma}$ in front of the integral defining $\tilde{\sigma}_{ij}^{\mathrm{Re}}$ is arbitrary, but must have an opposite sign with respect to $\mathcal{I}(0)$, namely, it must be negative for $\alpha < 1/2$ and positive for $\alpha > 1/2$, as illustrated in Fig. 5(a) plotting $\mathcal{I}(0)$ versus α. Figure 5(b) displays the ratio $\delta\theta^2/(\eta\tilde{\gamma}\mathcal{I}(0))$ versus α [see Eq. (56)].

The velocity component u can now be expressed from Eq. (D15) and the component v from

$$v'(\theta) = -\frac{\eta U}{\delta\theta}\tilde{g}_1''(\tilde{\theta})\theta, \tag{D28}$$

where we set $\sin\theta \approx \theta$. It follows that v is of order $\eta^{3/2}$, although u is bigger, of order η (the integration over θ amounts to multiply the prefactor $\eta U/\delta\theta$ by $\delta\theta$). Inserting in Eq. (D17) the relations (D22) and (D25), and defining $k = \delta\theta^2/\eta$ in Eq. (56), the integration of Eqs. (D15) and (D28) gives the velocity profiles

$$u(\theta) - U = \frac{\eta U}{d_\alpha}\int_0^{\theta/\theta_c} dy\,(1+y^2)^{-1/\alpha} \tag{D29}$$

and

$$v(\theta) - v(0) = \frac{\eta U\theta_c}{d_\alpha}\int_0^{\theta/\theta_c} dy\,y(1+y^2)^{-1/\alpha}, \tag{D30}$$

where $\theta_c = \tilde{\theta}_c\delta\theta = \tilde{\theta}_c\sqrt{k\eta}$, which gives

$$v(\theta) = -\frac{\eta^{3/2}Uk^{1/2}\tilde{\theta}_c}{d_\alpha}\,\frac{\alpha}{2(1-\alpha)}\left(1+\frac{\theta^2}{\theta_c^2}\right)^{-\frac{1-\alpha}{\alpha}}, \tag{D31}$$

where

$$k = \tilde{\gamma}\mathcal{I}(0)\,\frac{4}{\tilde{\theta}_c^2}\,\frac{1-\alpha}{\alpha}\,\frac{c_\alpha}{d_\alpha}$$

is a positive constant because the product $\tilde{\gamma}\mathcal{I}(0)$ has to be positive.

APPENDIX E: COMPARISON WITH THE MIXING LAYER EXPERIMENT OF SODJOVI

Let us first recall that when using the Boussinesq model for turbulent stress tensor, ($\sigma^{\mathrm{Re}} = \nu_t u_{,y}$ where the turbulent viscosity ν_t is a linear function of x, independent of y), one finds that the width of the turbulent domain scales as η for small values of this ratio η [12–14]. In the literature we found few experimental works devoted to small values of η, most of them being concerned by ratios U_1/U_2 of order of a few units. Nevertheless, we found in Ref. [12] a measurement extending from $\eta = 0.05$ up to $\eta = 0.6$ which displays a peculiar nonlinear behavior of the curve $\delta\theta$ versus η, at small η values, although the author concludes that the width of the turbulent domain grows linearly with η in agreement with the Boussinesq model.

Using the data published in Table 3.2 of Ref. [12] we have plotted $\delta\theta$ versus $\eta^{1/2}$ (see Fig. 6). It appears that the plot agrees quite well with our prediction [Eq. (51)], for η smaller than 0.26, which is not a small domain ($\eta = 0.26$ corresponds to $U_1 = 1.7U_2$).

From Fig. 6 we deduce the experimental value of the ratio $\delta\theta/\sqrt{\eta}$. The experiment provides $\sqrt{k} = 0.036$ defined in Eq. (56) or Eq. (D26), which allows to obtain a numerical value for the prefactor $\tilde{\gamma}$ in Eq. (3):

$$\tilde{\gamma}(\alpha) = k\frac{1-\alpha}{\alpha}\tilde{\theta}_c^2\frac{d_\alpha}{c_\alpha}\frac{1}{4\mathcal{I}(0)}. \tag{E1}$$

It depends on the exponent α, as illustrated in Fig. 7 (see caption for the divergence for $\alpha = 1/2$). Close to this peculiar value, one may use the approximation $\mathcal{I}(\theta - \theta') \approx \mathcal{I}(\delta\theta)$, or solve more precisely the equation $C + D = 0$, something not done here.

APPENDIX F: ORDER OF MAGNITUDE OF $\tilde{\sigma}_{ij}^{\mathrm{Re}}$

From Eq. (31) and the hypothesis $\mathcal{I}(\theta - \theta') = \mathcal{I}(0)$, we have

$$\tilde{\sigma}_{xx}^{\mathrm{Re}} = \tilde{\gamma}\rho\mathcal{I}(0)|g + g''(\theta)|^{1-\alpha}\int d\theta'\,|g + g''(\theta)|^{\alpha}\,\tilde{\tau}_{xx}(\theta'), \tag{F1}$$

where $\tilde{\tau}_{xx}(\theta') = (g + g'')\sin 2\theta'$ [see Eq. (28)]. Because $\tau_{xx} = -\tau_{yy}$ we have

$$\tilde{\sigma}_{xx}^{\mathrm{Re}} = -\tilde{\sigma}_{yy}^{\mathrm{Re}}. \tag{F2}$$

The nondiagonal element of the tensor $\tilde{\sigma}_{ij}^{\mathrm{Re}}$ is

$$\tilde{\sigma}_{xy}^{\mathrm{Re}} = \tilde{\gamma}\rho\mathcal{I}(0)|g + g''(\theta)|^{1-\alpha}\int d\theta'\,|g + g''(\theta)|^{\alpha}\,\tilde{\tau}_{xy}(\theta'), \tag{F3}$$

where $\tilde{\tau}_{xy}(\theta') = -(g + g'')\cos 2\theta'$ is an even function. Using the same argument as above, we have $\tilde{\sigma}_{xy}^{\mathrm{Re}} \sim \delta\theta(g'')^2$ or $\tilde{\sigma}_{xy}^{\mathrm{Re}} \sim \eta^{3/2}U^2$. The integral in Eq. (F3) does not vanish because the integrand is an even function; then

$$\tilde{\sigma}_{xy}^{\mathrm{Re}} \sim \eta^{3/2}. \tag{F4}$$

A priori the diagonal elements $\tilde{\sigma}_{xx}^{\mathrm{Re}} = -\tilde{\sigma}_{yy}^{\mathrm{Re}}$ are of order $(\delta\theta)^2(g'')^2 \sim \eta^2U^2$ under the condition that the integrand is even. But $\tilde{\tau}_{xx}$ is an odd function; then we have $\tilde{\sigma}_{xx}^{\mathrm{Re}} = -\tilde{\sigma}_{yy}^{\mathrm{Re}} = 0$ at order η^2. To go further we have to notice that the results of this section are obtained within the rough approximation $\mathcal{I}(\theta - \theta') = \mathcal{I}(0)$ which greatly simplifies the calculation. This approximation is valid for small values of the angles, except for $\alpha = 1/2$ where $\mathcal{I}(0) = 0$. This point is considered below.

1. Case $\alpha \neq 1/2$

More generally, close to $\theta = \theta'$, for any α values we have shown in Eq. (36) that

$$\mathcal{I}(\theta - \theta') \approx \mathcal{I}(0) + b|\theta - \theta'|, \tag{F5}$$

where b is a factor quasi-independent of α ($b \approx 9$), whereas $\mathcal{I}(0)$ changes a lot with α [more precisely it grows from -5 up to 25 when α increases from $-1/4$ to $3/4$; see Fig. 2(b)]. The second term in Eq. (F5) changes the above results as follows: all odd terms which have been considered as providing a null contribution to the integral over θ' in $\sigma_{ij}^{\mathrm{Re}}$ will now bring a nonzero contribution and provide a component having an order of magnitude equal to the same order of magnitude as before times $b\delta\theta \sim \eta^{1/2}$ [the approximate value of $\mathcal{I}(\theta - \theta')$] for small argument. In summary, for $\alpha \neq 1/2$ we get

$$\left\{\begin{array}{l} \tilde{\sigma}_{xx}^{\mathrm{Re}} = -\tilde{\sigma}_{yy}^{\mathrm{Re}} \sim \eta^{5/2} \\ \tilde{\sigma}_{xy}^{\mathrm{Re}} \sim \eta^{3/2} \end{array}\right\} \tag{F6}$$

which confirms that the tensor $\tilde{\sigma}_{ij}^{\mathrm{Re}}$ does not satisfy the realizability conditions

$$\left\{\begin{array}{ll} \sigma_{ii} \geqslant 0 & \\ \sigma_{ij}^2 \leqslant \sigma_{ii}\sigma_{jj} & \text{for} \quad i \neq j \end{array}\right\}. \tag{F7}$$

Indeed both conditions in Eq. (F7) are not fulfilled; one diagonal element of $\tilde{\sigma}$ is negative, moreover, Eq. (F6) show that the orders of magnitude of the components are inconsistent with the Schwarz inequality, a binding constraint of the Reynolds stress defined by Eq. (1).

2. Case $\alpha = 1/2$

In the case $\alpha = 1/2$, one has $\mathcal{I}(0) = 0$ and $\mathcal{I}(\theta - \theta') \approx b\sqrt{1 - \cos(\theta - \theta')} \sim b|\theta - \theta'|$ where $b \approx 8.9$. For the tensor σ_{xx}^{I}, the components are respectively of order

$$\left\{\begin{array}{l} \tilde{\sigma}_{xx}^{\mathrm{Re}} = -\tilde{\sigma}_{yy}^{\mathrm{Re}} \sim \mathcal{I}(\delta\theta)(g'')^2\delta\theta \sin\theta \sim \eta^{5/2}U^2 \\ \tilde{\sigma}_{xy}^{Re} \sim \mathcal{I}(\delta\theta)(g'')^2\delta\theta \sim \eta^2U^2, \end{array}\right. \tag{F8}$$

which does not satisfy the realizability conditions because the second equation yields $\sigma_{xy}^2 > \sigma_{xx}\,\sigma_{yy}$ as in the general case of $0 < \alpha < 1$. But the realizability conditions are satisfied by adding the diagonal tensor (4) to the tensor $\tilde{\sigma}_{ij}^{\mathrm{Re}}$ because

$$\sigma_{ii}^{\mathrm{Re},p} \sim (\eta U)^2,$$

which is positive, of the same order as $\tilde{\sigma}_{xy}^{\mathrm{Re}}$, and satisfies the Schwarz inequality when taking $\gamma = \tilde{\gamma}$ as in the general case.

[1] J. Leray, Essai sur le mouvement d'un fluide visqueux emplissant l'espace, Acta Math. **63**, 193 (1934).

[2] Y. Pomeau, M. Le Berre, and T. Lehner, A case of strong nonlinearity: Intermittency in highly turbulent flows, C. R. Mec. **347**, 342 (2019), special issue on patterns and dynamics: Homage to Pierre Coullet.

[3] C. Josserand, Y. Pomeau, and S. Rica, Finite-time singularities as a mechanism for dissipation in a turbulent media, Phys. Rev. Fluids **5**, 054607 (2020).

[4] C. Josserand, M. Le Berre, and Y. Pomeau, Scaling laws in turbulence, Chaos **30**, 073137 (2020).

[5] To avoid the divergence of the integral over the Cartesian coordinate along the pipe (for instance) without introducing an arbitrary origin of coordinates one must restrict the choice of the Green's function to the relevant coordinates, namely, the ones entering in the dependence of the velocity field so that the integral on those relevant coordinates does not diverge *a priori*. In the case of a circular pipe flow the "relevant" coordinates are the two coordinates in the cross section of the pipe. In the case of a plane Poiseuille (or Couette) flow there is only one relevant coordinate, the one perpendicular to the two parallel limiting plates. The changes induced by this restriction to relevant coordinates concern both the number of dimensions and the dependence of the vector **X** (two dimensions in the case of a pipe flow and one for the plane Poiseuille flow).

[6] L. Landau and E. M. Lifshitz, *Course of Theoretical Physics, Fluid Mechanics* (Pergamon, Oxford, 1987).

[7] J. C. Maxwell, On the dynamical theory of gases, Originally published in the Philos. Trans. R. Soc. London **157**, 49 (1867), and in Philosophical Magazine **32**, 390 (1866), **35**, 129 (1868), **35**, 185 (1868); reprinted in *The Scientific papers of James Clerk Maxwell*, edited by W. D. Niven (Cambridge University Press, Cambridge 1890), Vol. 2, pp. 26–78.

[8] U. Schumann, Realizability of Reynolds-stress turbulence models, Phys. Fluids **20**, 721 (1977).

[9] H. Coanda, Device for deflecting a stream of elastic fluid projected into an elastic fluid, U.S. Patent No. 2,052,869 (1936).

[10] J. O. Hinze, *Turbulence* (McGraw-Hill, New York, 1975); see also more recent books by J. Mathieu and J. F. Scott, *Turbulent Flows: An Introduction* (Cambridge University Press, Cambridge, 2000) and references herein especially on RANS; P. Saut and C. Cambon, *Homogeneous Turbulence Dynamics*, 2nd ed. (Springer, Berlin, 2018); and for near wall turbulence see T. J. Craft and B. E. Launder, Application of TCL modelling to stratified flows, in *Closure Strategies for Turbulent and Transitional Flows*, edited by B. E. Launder and N. Sandham (Cambridge University Press, Cambridge, U.K., 2002).

[11] B. E. Launder, G. J. Reece, and W. Rodi, Progress in the development of a Reynolds stress turbulence closure, J. Fluid Mech. **68**, 537 (1975).

[12] K. Sodjavi, Etude expérimentale de la turbulence dans une couche de mélange anisotherme, Thesis, Université de Rennes 1, 2013, https://tel.archives-ouvertes.fr/tel-00921507.

[13] R. D. Metha, Effect of velocity ratio on plane mixing layer development: Influence of splitter plate wake, Exp. Fluids **10**, 194 (1991).

[14] H. Schlichting and K. Gersten, *Boundary Layer Theory* (Springer, Berlin, 1999).